Reliability study of PCB-embedded power dies using solderless pressed metal foam

Said Bensebaa, Mounira Bouarroudj-Berkani, Stéphane Lefebvre, Mickael Petit, Nicolas Schmitt, Shuanfeng Zhang

Version of Record: https://www.sciencedirect.com/science/article/pii/S0026271420304789
Manuscript_c34f39cb725f5a98f6aed94665e772c3

Reliability Study of PCB-Embedded Power Dies Using Solderless Pressed Metal Foam

S. Bensebaa, M. Berkani, S. Lefebvre, M. Petit, N. Schmitt, S. Zhang

Abstract – This paper presents a reliability study of an innovative process of embedding power dies in PCBs. Firstly, a description of this solderless package is given. Secondly, experimental tests of thermal aging for the proposed package are performed through passive thermal cycling in the range of PCB standards. Thirdly, a 2D finite element model of the package is built using material properties obtained from previous thermomechanical characterizations. Numerical simulations of a passive thermal cycling of the package are carried out. The analysis of the strain-stress fields allows to highlight the time-space areas where they are critical and compromise the reliability.

1. Introduction

The classical power module packaging, that uses solders and wire bonding, presents several limitations such as large stray inductance (ten to several dozen nH) which can be critical for high speed component like wide band gap devices (GaN HEMT and SiC MOSFETs) [1]. Wireless bonding technologies based on sintering or soldering the back side and electroplating the top side of the die were developed [2-4]. In [5-6] an embedding power die on PCB is presented where a pressed metal foam has been used on the top side and solder joint on the back side. The reliability experimental investigation of this packaging was performed [7], in which samples were thermally cycled between (–40 °C and 150 °C). In this study, a reliability of an enhancement of the previous process of embedding power die on PCB that uses only pressed metal foam without solder is presented. Realized samples are subjected to a thermal cycling protocol according to PCB standards thermal conditions [JESD22-A104E, MIL-STD-883E]. Moreover a FEM simulation of the package is implemented in order to evaluate thermomechanical stresses occurring during ageing conditions and to present the most critical areas of the assembly in terms of reliability.

2. Packaging choices and process

The manufacturing process of the packaging is simple and can be described in two stages.

The first stage consists of stacking layers starting with:

- Bottom PCB, composed of Copper and Epoxy FR4 layers (Cu 35 µm Epoxy 400 µm), ref: ABC16;
- Uncured Prepreg layers with a hole with die dimensions; these layers being composed of 49%wt epoxy resin and 51%wt fiberglass, which are cured by applying high temperature and pressure conditions, ref: Panasonic R-1650V;
- Bottom metal foam;
- Epoxy FR4 with a hole with die dimensions, it is used to keep the die fixed during pressing process;
- Power die; for this study an Infineon diode with dimensions of 7,3 x 7 x 0,11 mm was used, ref: Infineon IDC51D120T6M.

Then symmetrically the deposition of the same layers are repeated:

- Prepreg layers;
- Top metal foam;
- Top PCB layer, Fig. 1 (b).

The second stage consists of pressing and curing the stack of layers under specified pressure and temperature conditions that are recommended by the Prepreg layer constructor using (LPKF MultiPress S).

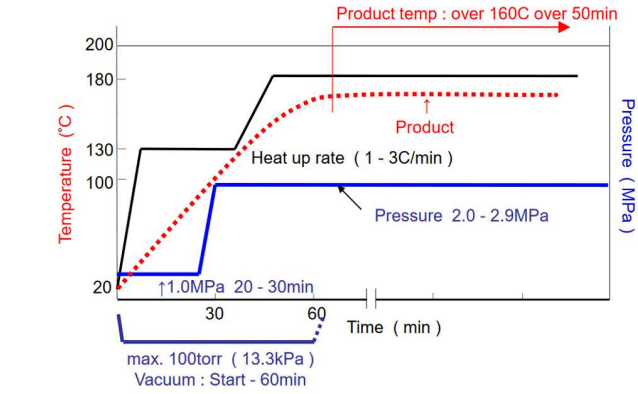

(a)

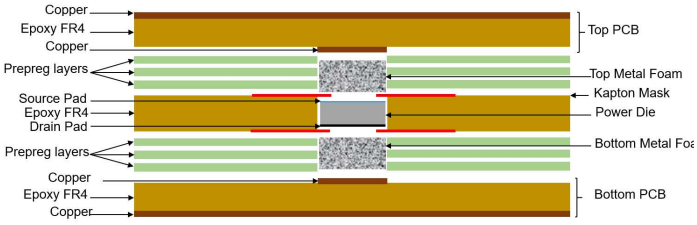

(b)

Fig. 1. (a) General recommendations of pressure and temperature conditions for press machine [8], (b) Manufacturing process of embedding power diode using pressed metal foam.

Note that a polyimide mask is added in order to have a specified surface of contact between foam and die. It allows to prevent an equipotential near the guard rings on the top side of the die. This polyimide layer can also be used to separate the gate from the source in case of transistors integration. The obtained device is shown in Fig. 2 (a) where SEM micrograph shows the detail of the packaging with a zoom on die-pressed foam contact region.

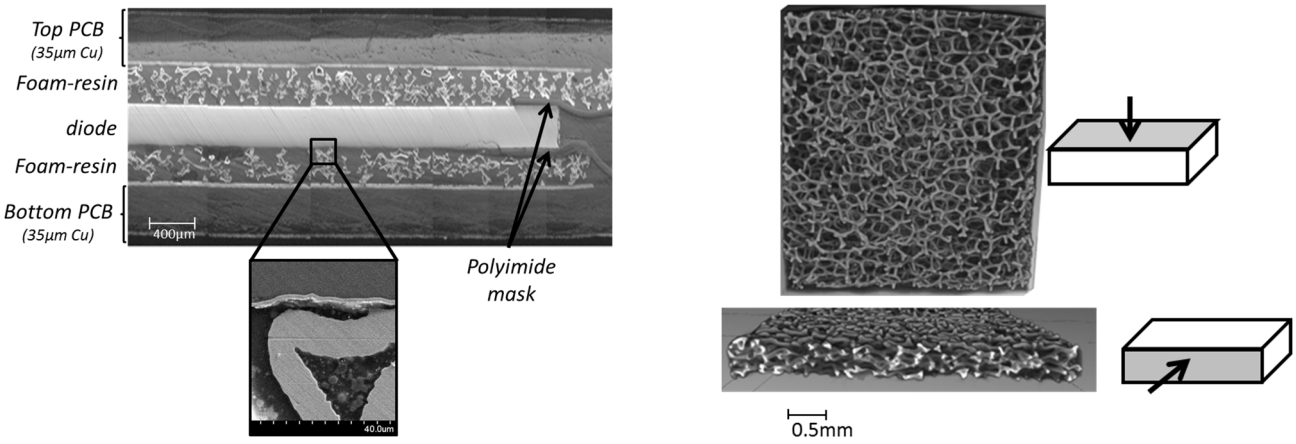

(a) (b)

Fig. 2. Microscopic section view of an embedded die using Nickel foam as top and bottom contacts with a zoom on the bottom die contact (a), Tomographic analysis showing the microstructure of the RIMF metal part (b).

3. Material characterization

Die contacts in the proposed packaging are made of resin-impregnated metal foam (RIMF). Two types of metal foam have been tested: Copper foam (ref: Cu-4753.0,13) and Nickel foam (ref: Ni-4753.0,13). 3D imaging of the bulk of RIMF was done by x-ray µCT. Images highlight the porous and inhomogeneous structure of the obtained mixture, Fig. 2 (b).
Electrical and thermal experimental characterizations of the RIMF have been made. The summary of the results brings us to the conclusion that Copper foam on the bottom side leads to a better heat release and Nickel foam on the top side contact leads to less electrical contact resistance [9]. Here we will detail only thermo-mechanical characterization. Even if the RIMF exhibits an elasto-plastic behaviour, this previous study was limited to the identification of the thermoelastic properties of the RIMF.

3.1. Coefficient of thermal expansion of foam-resin mixture

The coefficient of thermal expansion (CTE) α_i in direction x_i was measured using a NETZSCH TMA 402 F1 Hyperion, thermomechanical analyser, by applying a temperature change $\Delta T = T - T_o$ with T between 200 and -50°C and $T_o = 25$°C on the characterized sample and measuring the length change $\Delta l_i = l_i - l_{oi}$. Equation 1 gives the relationships.

$$\alpha_i(\mathrm{T}) = \frac{\varepsilon_i^{th}}{\Delta T} \quad \text{with} \quad \varepsilon_i^{th} = \frac{\Delta l_i}{l_{oi}} \tag{1}$$

Along the *z*-axis, the CTE is around 5×10^{-5} K^{-1}, from -50°C and 100°C. Then it increases, first slowly up 70 ppm/°K at 150°C and finally abruptly between 150°C and 200°C reaching 250 ppm/°K at 200°C goes over 250 ppm/°K, once the glass transition temperature (Tg) of the Epoxy is reached. For *x*, *y*-axes the CTE is around 46 ppm/°K. So, the maximum operating temperature of the assembly should not exceed Tg of the resin epoxy.

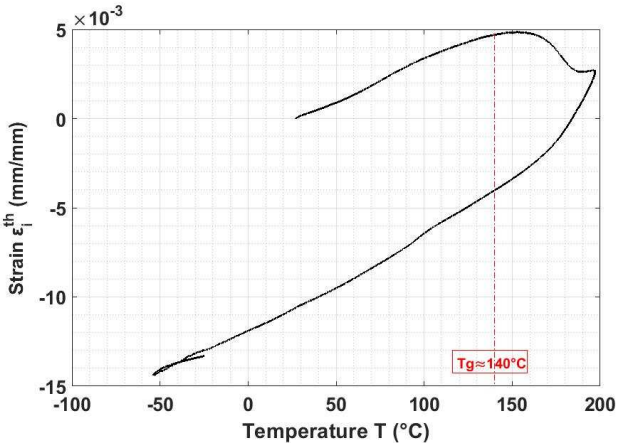

Fig. 3 Dilatometry test for CTE measurement along the z-axis versus temperature for pressed Nickel RIMF.

3.2 Elastic properties of foam-resin mixture

The elastic properties in the three directions x_i and for several temperatures were characterized using the same thermomechanical analyser on prismatic samples with lateral size of 6 mm and a maximal length of $l_{oi} = 0{,}79$ mm. Compression loading-unloading tests were performed by applying a load F lower than 3 N to ensure the sample remains elastic. The normal stress is computed by $\sigma_{ii} = F/S_i$ and the associated normal strain $\varepsilon_{ii} = \Delta l_i / l_{oi}$ from the measure of the sample length change $\Delta l_i = l_i - l_{oi}$. From both measures the Young's Modulus E_i in the direction x_i is deduced, Equation. 2.

$$E_i(\mathrm{T}) = \frac{\sigma_{ii}}{\varepsilon_{ii}} \tag{2}$$

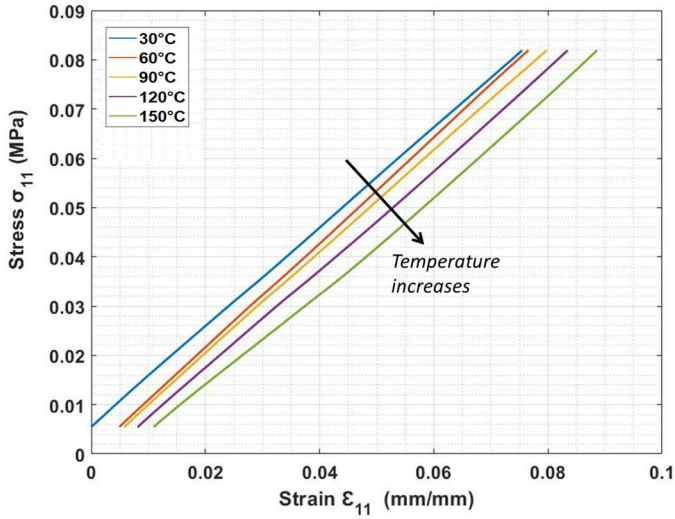

Fig. 4. Stress-strain diagram for a RIMF for different temperatures, in the z-axis. Only the loading steps is shown at each temperature and the maximal stress was limited to 0,082 MPa.

Tests were carried out at several temperatures below 150°C. For each successive temperature, a compression loading-unloading test was applied then the temperature was increased to the next target. As shown in Fig. 4, the temperature doesn't affect the Young's Modulus in the considered temperature range.

Because of the low load values that can be applied by the thermomechanical analyser, we have encountered problems related to the low stiffness of the contacts between the sample and the plates and therefore the values of Young's modulus is too low compared to what we should have expected with such a mixture. Indeed, with a mixture of madding with resin (Young's modulus of 3.5GPa) and Copper (131GPa) we should find a value between these two ones. Consequently, we used a numerical characterization method using a 3D geometric microstructure model obtained from the tomographic analysis and calculated the Young's modulus.

Obtained results show that the thermomechanical properties are the same whatever the nature of the foam, because the resin content is high in the obtained mixture and therefore it controls the mechanical behavior.

4. Experimental setup and ageing conditions

4.1. Approaches and accelerated ageing tests

In this part passive thermal cycling was performed using a thermal conditioner. The purposes of this study were first to evaluate the reliability of the proposed packaging under temperature cycles, then to analyse failures occuring after thermal aging.

Two thermal profiles have been used. The first one, cycle#1, in the range of -40°C and 140°C, with a cycle time of 30 minutes, which corresponds to a dwell time of 10 minutes and heating and cooling temperature ramps of 18°C/min. This profile is quite severe but allows to compare the behavior of the proposed packaging to those already developed based on the use of solder as a bottom connection [7]. The second one, cycle#2, is in the range of -25°C to 125°C with the same dwell time as cycle#1 but temperature ramps of 15°C/min. This profile is in the range of PCB standards [JESD22-A104E, MIL-STD-883E]. Before the thermal cycle tests, the die forward resistance was measured using a curve tracer in order to have the initial value. The resistance represents the slope of the curve $I_F = f(V_F)$, at a current of 40A. The initial electrical resistance of these packages was measured and is between 8 to 12 mΩ. During ageing the resistance was regularly monitored with a step of five cycles in order to follow its evolution finely.

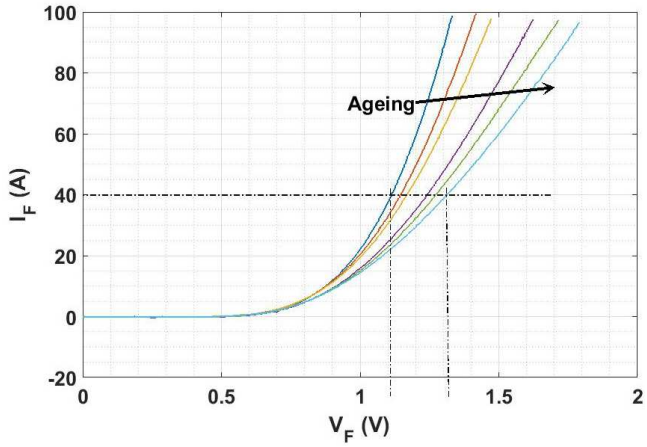

Fig. 5. Variations of the forward characteristics $I_F = f(V_F)$ with ageing under specified thermal cycling (cycle#1), from 0 to 25 cycles with a step of 5 cycles.

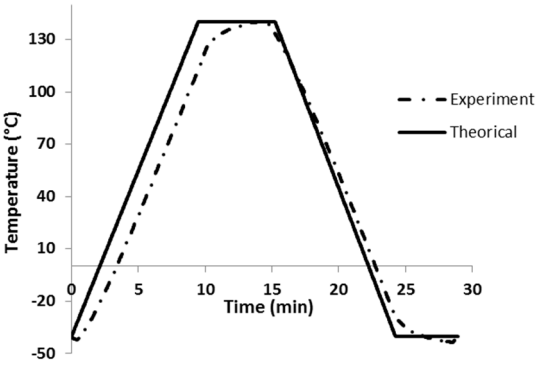

Fig. 6. Temperature cycles (cycle#1) between -40°C and +140°C. It was checked using thermocouples that the DUT is subject to the temperature set.

4.2. Experimental results

For devices aged under cycle#1 it can be observed that the forward resistance of the die regularly increases until failure. Indeed, a failure occurs for the most of the samples after only 40 to 50 cycles. These results are quite similar than that obtained with devices using solder [10].

In Fig. 7 a SEM micrograph of a sample is depicted after its failure. It reveals a significant delamination of the PCB's copper and cracks on the power die. As the maximum temperature exceeded the glass transition temperature (Tg) of

the Epoxy (around 130.-140°C), the thermal strains within the PCB are crucial. Consequently this thermal profile is not adequate for reliability analysis under passive thermal cycling.

Fig. 7. SEM cross-sectional view of a sample after failure (thermally aged under cycle#1)

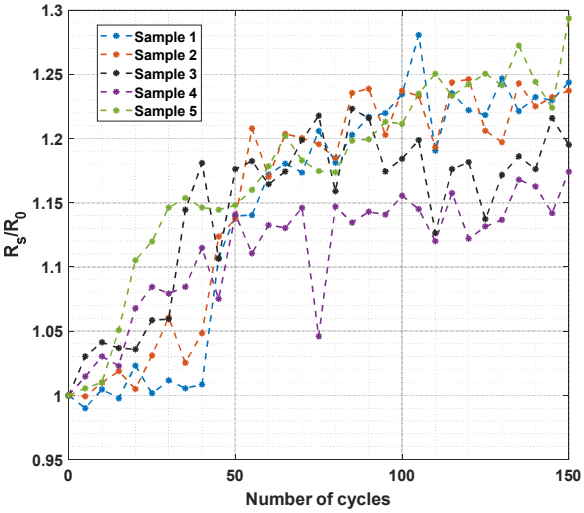

Fig. 8. Evolution of the standardized resistances of the different samples during the ageing process.

Under test condition of cycle#2, the components still operated after 160 cycles. As a result, evolutions of measured resistances during thermal cycling for the tested devices are depicted on Fig. 8. It shows that from the beginning of ageing forward resistance increased rapidly until around 15-20% after about the first fifty cycles then the growth rate decreased. The diode inside the package remained always operational after 160 cycles. It seems that the resistance of all packages change with a similar pattern and tend to stabilise with the rise of cycle number. To find out the cause of the resistance increase, a metallurgical cut was performed for a functional sample that passes 160 cycles using optical microscope but no sign of degradation was identified. Obtained results from the thermal cycling under both profiles are summarized in Table 1. A short dwell time was chosen in this study, because it is supposed that the creep effect is neglected when contacts are made with foam-resin mixture comparing to solder contact, which makes the proposed solution more beneficial.

5. Thermomechanical simulations

In order to understand the experimental test results, thermo-mechanical simulations of the packaging were carried out using finite element analysis (FEA). The objective was to highlight the effects of temperature variations and to locate the stress concentration on the proposed packages.

Table 1: Thermal ageing results summary

	Nbr of DUT	ΔT (°C)	Cycles to failure
Cycle#1 (-40°C/140°C)	5	180	Around 50
Cycl#2 (-25°C/125°C)	17	150	> 160

5.1. 2D simulation models

The objective of these simulations was only to analyse qualitatively the thermomechanical stresses in two different packaging during thermal cycling. In the first numerical model solder are used to connect the bottom side of the die and a pressed Nickel foam to connect the top side (Packaging#1). In the second one contact is performed with Nickel foam for both top and bottom sides (Packaging#2). To simplify the model, only 2D axisymmetric structures have been considered, Fig. 9. Material data are given in Table 2. From the mechanical point of view, the Epoxy (FR4), Si die and the RIMF were considered as elastic, copper metallization is considered with elasto-plastic properties and solder is considered as a elasto-viscoplastic material and modelled with the Garofalo model which parameters are given in table 2 [11].

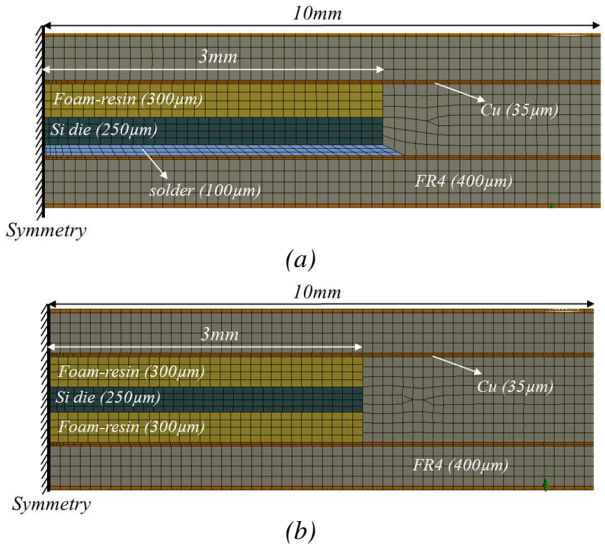

Fig. 9. Simulated geometries, (a) Model using metal foam on the top side and solder on bottom side, Packaging#1, and (b) Model with metal foam for both top and bottom side, Packaging#2.

Fig. 10 gives the Von Mises stress maps for simulated temperature profile (-40°C/140°C) where the maximum values are reached at 140°C. Notice that the "Von Mises" equivalent stress in the package that uses only the metal foam is lower than the one using metal foam and solder joint due to stress relaxation.

Table 2: Solder Garofalo parameters of Sn3.0Ag0.5C solder [11].

C (1/s)	*α* (1/MPa)	*n*	*Q/R* (K)
6.385e-6	0.08638	5.84	159.97

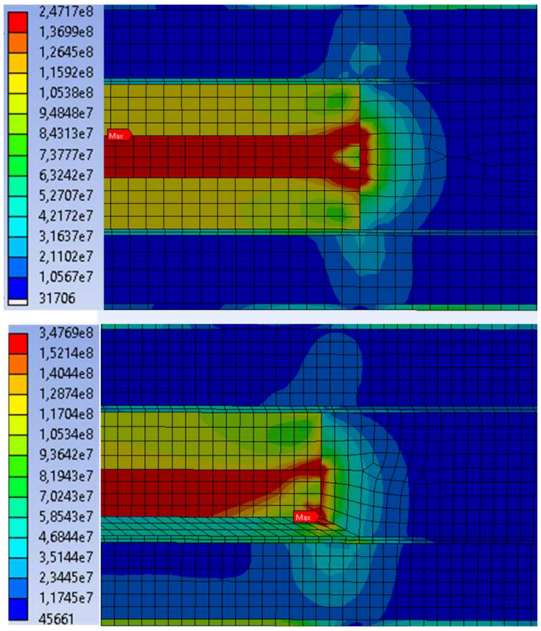

Fig. 10. Maps of maximum Von Mises stress (Pa) at T = 140°C for temperature profile from -40°C to 140°C

Results show that the maximum von Mises stress is located in the die at the solder and foam interfaces for the Packaging#1 while it is located in the die for the Packaging#2.

For more details, we plot the evolution of the maximum von Mises stress taken from the different layers of the modelled packaging as function of time. The results are depicted in Fig. 11, in solid lines are represented the results from the Pakaging#1 and in dotted line those from Packaging#2. It can be noted that the stress in all layers is higher for the packaging#1. Furthermore, replacing the solder with metallic foam reduces (by a factor of 1,4) the stresses in the chip.

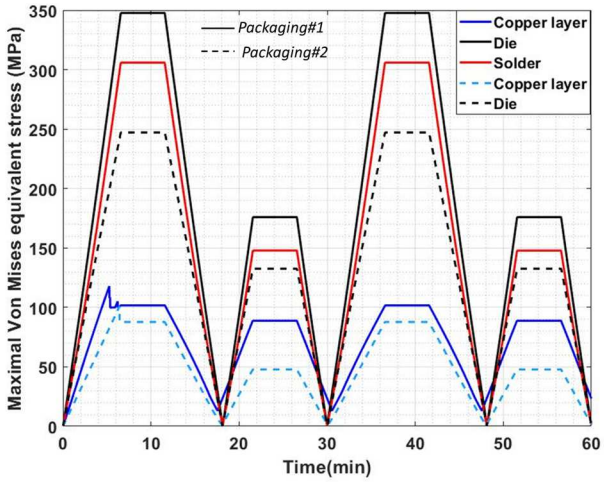

Fig. 11. Maximal Von Mises stress taken in modelled packaging in the die, copper and solder layers. Solid lines are from Packaging#1 (that using solder for bottom contact) and in dotted line results from Packaging#2 (with foam for all contacts).

5. Conclusion

This paper relates a first study on the reliability of power embedded die packaging based on pressed metal foam contacts without solder and bonding wires. First results of thermal cycling under PCB normative specifications ageing tests show a good reliability of the proposed packaging. Material characterizations have been performed in order to determine thermomechanical properties of the material formed by foam and resin mixture.

Thermomechanical simulations allow first estimations of the stress maps that are correlated to the reliability performances of the proposed package. The maximum stresses and strains within the package were located (only von Mises stress maps have been illustrated here). They show that replacing the solder attach in the case of a packaging with metal foam on the top side by the use of foam metal reduces the stress level in the die. As future work, it is planned to study the impact of chip size and thickness on performances and reliability of the proposed packaging.

Table 3. Material physical properties [11][12][13]

Materials	Thermal conductivity *(W/m.K)*	CTE *(ppm/K)*	Young's modulus *(GPa)*	Poisson's ratio	Yield strength *(MPa)*	Tangent modulus *(MPa)*
Copper	400	17	131	0,345	100	400
Sn3.0Ag0.5Cu	58.7	23	43	0,33	25.6	
Si	148	2.46	166	*0,42*		
Epoxy FR4	0.3	15 (x-axis) 17 (y-axis) 85 (z-axis)	17,9	0,17	*(elastic)*	
resin-Ni foam	1,9	48	33.7	0,3		
resin-Cu foam	5	48	33.7	0,3		

References

[1] A. Hamidi et D. Cottet, « Parasitics in power electronics packaging », IMAPS. Long Beach, California, USA: IMAPS, nov. 2004.

[2] D. J. Kearney, S. Kicin, E. Bianda, et A. Krivda, « PCB Embedded Semiconductors for Low-Voltage Power Electronic Applications », IEEE Transactions on Components, Packaging and Manufacturing Technology, vol. 7, no 3, p. 387-395, mars 2017.

[3] G. Regnat et al., « Silicon carbide power chip on chip module based on embedded die technology with paralleled dies », in 2015 IEEE Energy Conversion Congress and Exposition (ECCE), Montreal, QC, Canada, 2015, p. 4913-4919.

[4] Huazhong University of Science and Technology et C. Chen, « A Review of SiC Power Module Packaging: Layout, Material System and Integration », CPSS Transactions on Power Electronics and Applications, vol. 2, nº 3, p. 170-186, sept. 2017, doi: 10.24295/CPSSTPEA.2017.00017.

[5] Y. Pascal, D. Labrousse, M. Petit, S. Lefebvre, and F. Costa, « PCB-Embedding of Power Dies Using Pressed Metal Foam », in Power Conversion, Intelligent Motion (PCIM), Nuremberg, 2018.

[6] Y. Pascal, A. Abdedaim, D. Labrousse, M. Petit, S. Lefebvre, et F. Costa, « Using Laminated Metal Foam as the Top-Side Contact of a PCB-Embedded Power Die », IEEE Electron Device Lett., vol. 38, no 10, p. 1453-1456, oct. 2017

[7] Y. Pascal, D. Labrousse, M. Petit, S. Lefebvre, et F. Costa, « Experimental investigation of the reliability of Printed Circuit Board (PCB)-embedded power dies with pressed contact made of metal foam », Microelectronics Reliability, vol. 88-90, p. 707-714, sept. 2018.

[8] Panasonic Corporation, Process Guidelines, «https://industrial.panasonic.com/content/data/EM/PDF/processguideline_R-1766GH.pdf»

[9] S. Bensabaa, M. Berkani, S. Lefebvre, M. Petit, « Design And Characterization Of PCB-Embedded Power Dies Using Solderless Pressed Metal Foam », Accepted at PCIM 2020,

[10] Y. Pascal, « Étude multicritère pour l'enfouissement partiel ou total de convertisseurs d'électronique de puissance dans un circuit imprimé », Université Paris-Saclay, 2019. Français. ⟨NNT : 2019SACLN038⟩.

[11] Zhang L, He JHC. Reliability behavior of lead-free solder joints in electronic components. Mater Electron 2013:172–90. doi:10.1007/s10854-012-0720-y.

[12] J.F. Shackelford and W. Alexander, "Materials scienceandengineering handbook", CRC Press, 2001.

[13] Arlon," Electronic Materials", Available online « http://www.arlonemd.com/products/».

[14] J. Skibinski, K. Cwieka, S. Haj Ibrahim, et T. Wejrzanowski, « Influence of Pore Size Variation on Thermal Conductivity of Open-Porous Foams », Materials, vol. 12, nº 12, p. 2017, juin 2019, doi: 10.3390/ma12122017.

[15] G. Girard et al., « Experimental and numerical characterization of thin woven composites used in printed circuit boards for high frequency applications », Composite Structures, vol. 193, p. 140-153, juin 2018, doi: 10.1016/j.compstruct.2018.03.037.

[16] C. Yu, « Technologies for integrated power converters », Electric power Université Paris-Saclay,2016. ⟨NNT:2016SACLS485⟩. ⟨tel-01445404⟩

[17] T. Stockmeier, P. Beckedahl, C. Gobl, et T. Malzer, « SKiN: Double side sintering technology for new packages », in 2011 IEEE 23rd International Symposium on Power Semiconductor Devices and ICs, San Diego, CA, USA, mai 2011, p. 324-327, doi: 10.1109/ISPSD.2011.5890856.

[18] L. Xu, Y. Zhou, et S. Liu, « DBC substrate in Si- and SiC-based power electronics modules: Design, fabrication and failure analysis », in 2013 IEEE 63rd Electronic Components and Technology Conference, Las Vegas, NV, USA, mai 2013, p. 1341-1345, doi: 10.1109/ECTC.2013.6575747.

[19] W. Kpobie et al., « Thermo-mechanical simulation of PCB with embedded components », Microelectronics Reliability, vol. 65, p. 108-130, oct. 2016, doi: 10.1016/j.microrel.2016.08.016.

[20] A. Salahouelhadj, M. Martiny, S. Mercier, L. Bodin, D. Manteigas, et B. Stephan, « Reliability of thermally stressed rigid–flex printed circuit boards for High Density Interconnect applications », Microelectronics Reliability, vol. 54, nº 1, p. 204-213, janv. 2014, doi: 10.1016/j.microrel.2013.08.005.